Cell PRESS
Open ACCESS

Cell Reports
Report

FLT3-ITDs Instruct a Myeloid Differentiation and Transformation Bias in Lymphomyeloid Multipotent Progenitors

Adam J. Mead,[1,*] Shabnam Kharazi,[3] Deborah Atkinson,[1] Iain Macaulay,[1,2] Christian Pecquet,[4,5] Stephen Loughran,[1] Michael Lutteropp,[1,2] Petter Woll,[1] Onima Chowdhury,[1] Sidinh Luc,[1] Natalija Buza-Vidas,[1] Helen Ferry,[1] Sally-Ann Clark,[1] Nicolas Goardon,[2] Paresh Vyas,[2] Stefan N. Constantinescu,[4,5] Ewa Sitnicka,[3] Claus Nerlov,[2,6] and Sten Eirik W. Jacobsen[1,2,*]

[1]Haematopoietic Stem Cell Biology Laboratory
[2]MRC Molecular Haematology Unit
Weatherall Institute of Molecular Medicine, University of Oxford, Oxford OX3 9DS, UK
[3]Hematopoietic Stem Cell Laboratory, Lund Stem Cell Center, Lund University, Lund 22184, Sweden
[4]Ludwig Institute for Cancer Research, Brussels B1200, Belgium
[5]de Duve Institute, Université Catholique de Louvain, Brussels B1200, Belgium
[6]Institute for Stem Cell Research, MRC Centre for Regenerative Medicine, University of Edinburgh, King's Buildings, West Mains Road, Edinburgh EH93JQ, UK
*Correspondence: adam.mead@imm.ox.ac.uk (A.J.M.), sten.jacobsen@imm.ox.ac.uk (S.E. W.J.)
http://dx.doi.org/10.1016/j.celrep.2013.04.031

SUMMARY

Whether signals mediated via growth factor receptors (GFRs) might influence lineage fate in multipotent progenitors (MPPs) is unclear. We explored this issue in a mouse knockin model of gain-of-function *Flt3-ITD* mutation because FLT3-ITDs are paradoxically restricted to acute myeloid leukemia even though Flt3 primarily promotes lymphoid development during normal hematopoiesis. When expressed in MPPs, Flt3-ITD collaborated with *Runx1* mutation to induce high-penetrance aggressive leukemias that were exclusively of the myeloid phenotype. Flt3-ITDs preferentially expanded MPPs with reduced lymphoid and increased myeloid transcriptional priming while compromising early B and T lymphopoiesis. Flt3-ITD-induced myeloid lineage bias involved upregulation of the transcription factor *Pu.1*, which is a direct target gene of Stat3, an aberrantly activated target of Flt3-ITDs, further establishing how lineage bias can be inflicted on MPPs through aberrant GFR signaling. Collectively, these findings provide new insights into how oncogenic mutations might subvert the normal process of lineage commitment and dictate the phenotype of resulting malignancies.

INTRODUCTION

Whether signals mediated via growth factor receptors (GFRs) might influence lineage fate in normal multipotent progenitors (MPPs) and stem cells remains unclear and disputed. New insights into this process have recently been gained through studies in vitro (Rieger et al., 2009); however, whether GFR signaling instructs lineage specification in vivo remains a key unresolved issue (Enver and Jacobsen, 2009). Studying the impact of gain-of-function mutations is an alternative approach to determine whether and how GFRs might instruct lineage fate in vivo. Indeed, activating mutations of GFRs and downstream signaling pathways are common events in cancer, particularly in hematopoietic malignancies such as acute myeloid leukemia (AML), and often show striking associations with distinct clinical and cell-lineage phenotypes (Croce, 2008). In some cases, this might simply reflect the fact that such mutations primarily target a specific cell lineage. However, more intriguingly, if a mutation targets a primitive multipotent cell, it might instruct lineage-fate decisions. As recent investigations of human AML have suggested that the propagating cell might frequently represent the counterpart of normal MPPs (Goardon et al., 2011), it is possible but still unclear to what degree GFR signaling mutations might also influence lineage specification in multipotent cells.

A good example of aberrant GFR signaling associated with specific leukemia phenotypes relates to the FMS-like tyrosine kinase 3 receptor (FLT3), which is expressed in the majority of cases of AML and acute lymphoblastic leukemia (ALL) (Stirewalt and Radich, 2003). Constitutively activating internal tandem duplications (ITDs) within the juxtamembrane domain of FLT3 occur in ~25% of cases of AML, conferring an adverse prognosis (Stirewalt and Radich, 2003). However, despite the high frequency of FLT3 expression in ALL and the key role of Flt3 in early lymphoid development (Sitnicka et al., 2002), including high-level Flt3 expression in lymphoid-primed MPPs (LMPPs) with combined lymphoid and myeloid potential (Adolfsson et al., 2005), FLT3-ITDs are rare in cases of ALL, occurring in <1% in larger series (Leow et al., 2011).

As is the case for most leukemic mutations, it is unclear how often FLT3-ITDs are a true initiating event in myeloid

malignancies. Indeed, a number of lines of evidence support the notion that FLT3-ITDs are often acquired secondarily to an initiating clonogenic event (Gale et al., 2008; Jan et al., 2012), although when involved in chronic myelomonocytic leukemia (CMML), they may indeed be the initiating mutation (Lee et al., 2007). Nevertheless, in line with the normal expression pattern of Flt3 (Adolfsson et al., 2005), results from studies in patients are compatible with the notion that FLT3-ITDs occur within the human MPP compartment (Levis et al., 2005) and are an essential driver mutation within the founding leukemic clone (Ding et al., 2012; Smith et al., 2012). Thus, even though FLT3-ITDs might occur secondarily to an initiating clonogenic event in many cases, these mutations occur in multipotent cells (Levis et al., 2005) and FLT3-ITD GFR signaling appears to be an essential requirement for leukemia propagation (Smith et al., 2012). It is possible, therefore, that FLT3-ITDs may act to dictate the lineage fate and phenotype of the resulting leukemia. Compatible with a role of Flt3-ITD signaling in lineage determination, two different knockin mouse models of *Flt3-ITD* have been reported to develop a myeloproliferative phenotype exclusively (Lee et al., 2007; Li et al., 2008). However, although it was recently suggested that Flt3-ITDs deplete hematopoietic stem cells (HSCs) (Chu et al., 2012), the key progenitor population that propagates FLT3-ITD-induced myeloid disease, as well as the cellular and molecular bases of their myeloid lineage bias, remains unclear.

Using a mouse knockin model of the *Flt3-ITD* mutation, we investigated the cellular and molecular mechanisms by which constitutive GFR signaling might subvert lineage specification in MPPs and alter the cell fate of early lymphoid progenitors, in order to explain the myeloid bias of the resulting leukemias.

RESULTS

Flt3-ITD Collaborates with *Runx1* Mutation to Induce Aggressive AML

To definitively determine whether physiologically expressed FLT3-ITD impacts the establishment of myeloid versus lymphoid leukemia development, we crossed $Flt3^{ITD/ITD}$ with $Runx1^{fl/fl}$ (Growney et al., 2005) and *Mx1-Cre* mice to induce *Runx1* deletion in MPPs. Importantly, *Runx1* loss-of-function mutation is associated with both lymphoid and myeloid leukemia (Grossmann et al., 2011; Schnittger et al., 2011). Unexpectedly, even without poly I:C induction, $Flt3^{ITD/ITD}Runx1^{fl/fl}Mx1\text{-}Cre^{+}$ mice developed a high-penetrance, short-latency acute leukemia (Figure 1A) characterized by marked leukocytosis, anemia, and thrombocytopenia (Figures S1A–S1C) and hepatosplenomegaly. Peripheral blood (PB) and bone marrow (BM) morphology resembled AML in all diseased mice (Figures 1B–1D), and myeloid lineage was confirmed by flow cytometry (Figures 1E and S1D). Development of ALL was never observed. Leukemias showed deletion of the Runx1 DNA-binding domain (Figure S1E). The uniform myeloid-lineage leukemias in $Flt3^{ITD/ITD}Runx1^{fl/fl}$ $Mx1\text{-}Cre^{+}$ mice demonstrate a key role for Flt3-ITD signaling in introducing a myeloid-lineage bias during leukemogenesis.

Flt3-ITDs Expand Myeloid-Biased LMPPs

We next investigated the cellular and molecular bases for FLT3-ITD-induced myeloid bias. As shown previously (Lee et al., 2007), the multipotent $Lin^{-}Sca1^{+}c\text{-}Kit^{+}$ (LSK) compartment was expanded in $Flt3^{ITD/ITD}$ mice (Figure 2A). We applied CD150 and CD48 to determine the nature of the expanded cells within the LSK compartment (Kiel et al., 2005), as Flt3-ITD is not detectable at the cell surface (Figure S2A). Notably, the expansion of LSKs was wholly attributable to a marked expansion of $LSKCD150^{-}48^{+}$ MPPs in 8- to 10-week-old $Flt3^{ITD/ITD}$ mice (Figures 2B and 2C), in line with the recent observation that Flt3-ITD may suppress the HSC compartment (Chu et al., 2012). Heterozygous ($Flt3^{ITD/+}$) mice had an intermediate phenotype between $Flt3^{+/+}$ and $Flt3^{ITD/ITD}$ mice (Figures S2B and S2C). High-level Flt3 expression in the normal LSK compartment defines LMPPs that lack self-renewal and megakaryocytic (Mk) and erythroid (E) potential but sustain lymphomyeloid capability (Adolfsson et al., 2005), a progenitor that is also implicated in human AML (Goardon et al., 2011). Because $Flt3^{high}$ LMPPs reside almost exclusively in the $LSKCD150^{-}48^{+}$ compartment (Figure S2D), we explored whether the expanded $LSKCD150^{-}48^{+}$ cells in *Flt3-ITD* mice had LMPP-like characteristics. As expected for LMPPs (Månsson et al., 2007), HSC- and MkE-affiliated gene expression was downregulated in $Flt3^{ITD/ITD}$ $LSKCD150^{-}48^{+}$ MPPs (Figures 2D, 2E, and S2E), and in line with the molecular data they possessed little or no Mk potential in vitro (Figure 2F). In contrast, myeloid-affiliated gene expression was upregulated in $Flt3^{ITD/ITD}$ $LSKCD150^{-}48^{+}$ cells (Figure 2G), paralleled by high granulocyte-macrophage (GM) potential in vitro (Figure 2H). Early lymphoid transcriptional programs were downregulated in both $Flt3^{ITD/ITD}$ and $Flt3^{ITD/+}$ $LSKCD150^{-}48^{+}$ MPPs (Figures 2I and 2J), paralleled by severely reduced B cell potential in vitro (Figure 2K). Importantly, the lymphoid transcriptional program was already suppressed in $Flt3^{ITD/ITD}$ $LSKCD150^{-}48^{+}$ MPPs in embryonic day 15 (E15) fetal liver (FL) (Figure S2F), at which time the phenotype and number of $LSKCD150^{-}48^{+}$ MPPs were unaffected (Figure S2G). In keeping with this suppression of early lymphoid programs in fetal MPPs, the number of $B220^{+}CD19^{+}$ B cells was suppressed in *Flt3-ITD* E15 FL (Figure S2H), preceding the emergence of a myeloproliferative phenotype at this early stage of ontogeny (Figure S2I). This supports the notion that lymphoid suppression and myeloid bias in MPPs occurs as a cell-intrinsic and direct consequence of Flt3-ITD signaling.

Because FLT3-ITDs in humans often occur secondarily to an initiating clonogenic event (Jan et al., 2012), it is possible that in such cases it is the other genetic events and not the FLT3-ITD that influence the leukemic phenotype. In order to address this issue, we used *Vav-Cre* mediated recombination to examine the impact of *Runx1* loss of function on lineage priming in MPPs in the absence of Flt3-ITD. The data obtained demonstrate a significant upregulation of *Il7r* and *Rag1* expression in MPPs with no significant impact on *sIgH* expression (Figure S2J). This finding is in keeping with the high incidence of lymphoid malignancies in mouse models of *Runx1* mutation (Jacob et al., 2010; Kundu et al., 2005; Putz et al., 2006) and contrasts markedly with the suppression of lymphoid programs caused by Flt3-ITDs in MPPs. This supports the notion that it is GFR signaling through Flt3-ITD that instructs the uniform myeloid phenotype of leukemias resulting from the collaboration between Runx1 deletion and FLT3-ITD in LMPPs.

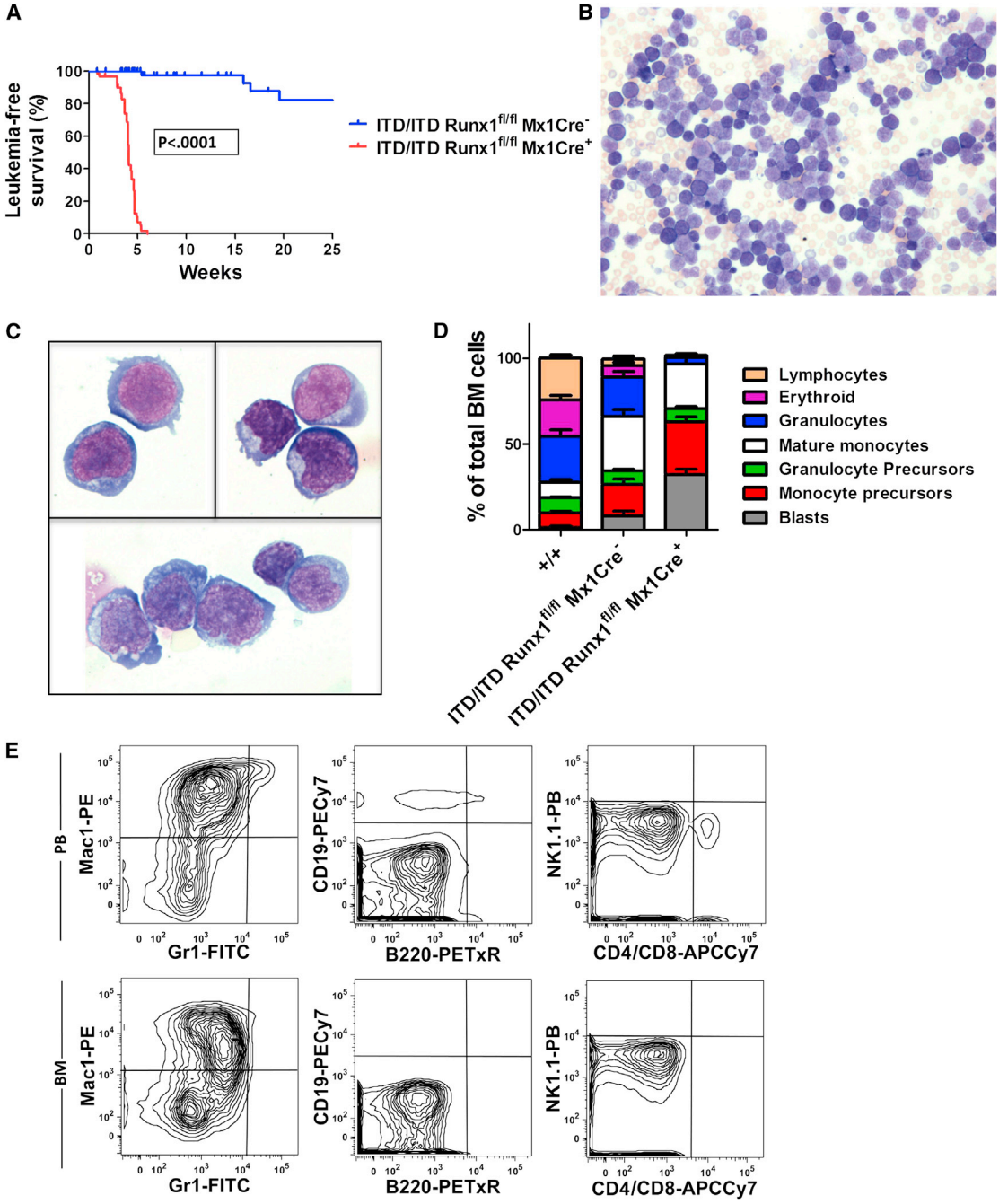

Figure 1. Mutation of *Runx1* in *Flt3*$^{ITD/ITD}$ Mice Results in High-Penetrance Aggressive Myeloid Leukemia

(A) Leukemia-free survival curves of *Flt3*$^{ITD/ITD}$*Runx1*$^{fl/fl}$ mice stratified according to *Mx1Cre* genotype (n = 50–68 mice of each genotype).

(B and C) Low-power (20×; B) and high-power (100×; C) morphology of typical leukemic cells in *Flt3*$^{ITD/ITD}$*Runx1*$^{fl/fl}$*Mx1Cre*$^{+}$ mice.

(D) Differential morphology results from BM of WT (+/+), *Flt3*$^{ITD/ITD}$*Runx1*$^{fl/fl}$*Mx1Cre*$^{-}$, and leukemic *Flt3*$^{ITD/ITD}$*Runx1*$^{fl/fl}$*Mx1Cre*$^{+}$ mice; percentage of total BM cells. Mean (SEM) values for 4–11 mice of each genotype.

(E) Fluorescence-activated cell sorting (FACS) analysis of PB and BM from an *Flt3*$^{ITD/ITD}$*Runx1*$^{fl/fl}$*Mx1Cre*$^{+}$ mouse with myeloid leukemia (representative of 19 further analyzed cases).

Error bars represent SEM. See also Figure S1.

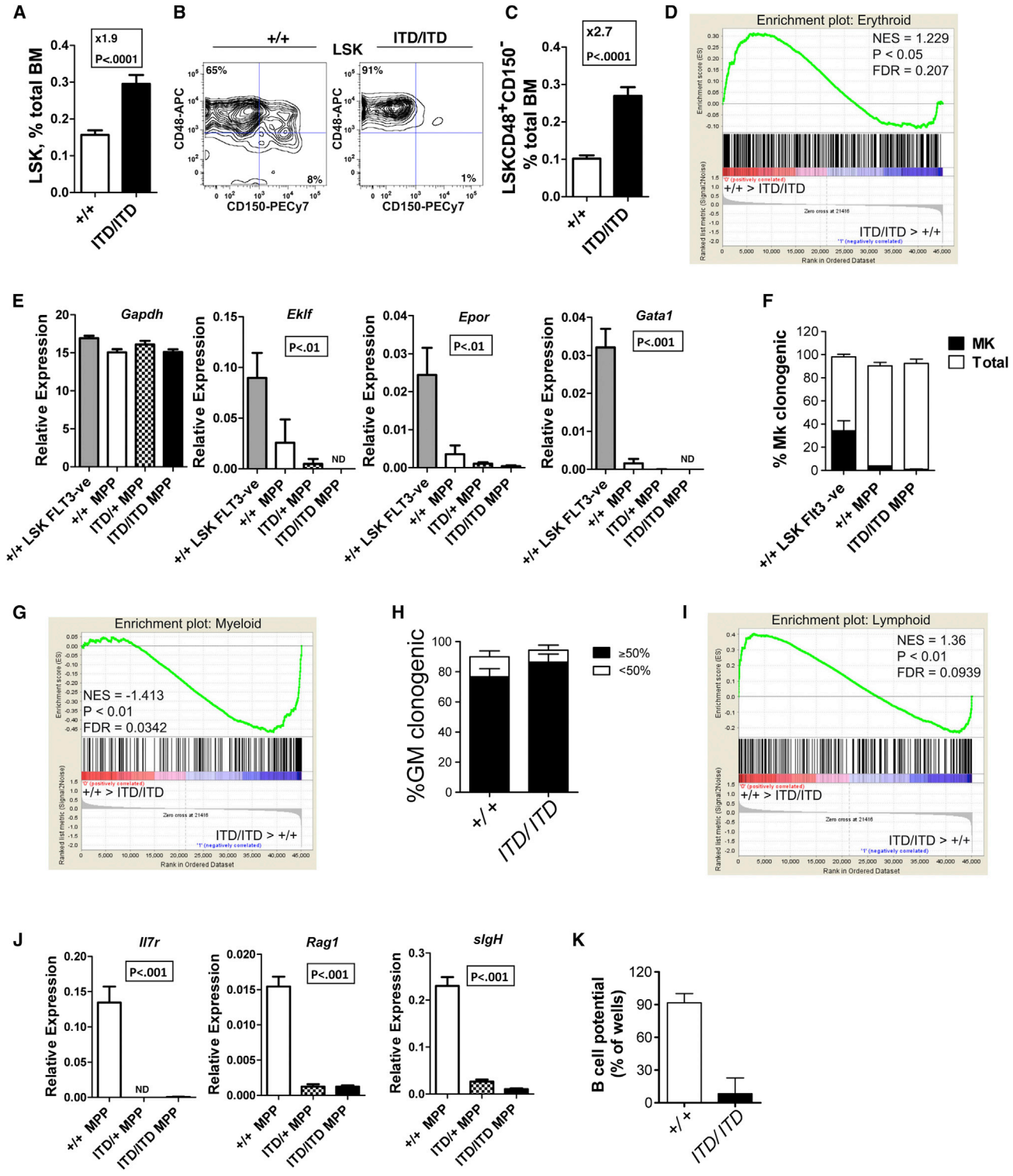

Figure 2. Flt3-ITDs Expand Myeloid-Biased MPPs

(A) Expansion of LSK cells in 8- to 10-week-old *Flt3*$^{ITD/ITD}$ mice (+/+: n = 27; ITD/ITD: n = 23).

(B) Expression of CD48 and CD150 on BM LSK cells from *Flt3*$^{+/+}$ and *Flt3*$^{ITD/ITD}$ mice.

(C) Expansion of LSKCD48^{+}CD150^{-} MPPs in 8- to 10-week-old *Flt3*$^{ITD/ITD}$ mice (+/+: n = 27; ITD/ITD: n = 23).

(D) GSEA demonstrating downregulation of E-affiliated genes in *Flt3*$^{ITD/ITD}$ versus *Flt3*$^{+/+}$LSKCD48^{+}150^{-} MPPs (n = 4 of each genotype). FDR, false discovery rate; NES, normalized enrichment score.

(legend continued on next page)

Flt3-ITD Suppresses Early T- and B-Lymphoid Progenitors

Because *Flt3-ITD* compromised lymphoid-transcriptional priming in LMPPs, which have been implicated as critical thymus-seeding progenitors (Luc et al., 2012), we next investigated whether T lymphopoiesis might be suppressed in *Flt3-ITD* mice. Thymic cellularity was found to be progressively reduced, and the earliest thymic progenitors (double-negative 1 Kit+ [DN1Kit$^+$]) were almost completely lost in *Flt3*$^{ITD/ITD}$ mice (Figures 3A–3C). Also, subsequent stages of DN2Kit$^+$ and DN3 thymocyte progenitors were severely reduced (Figures S3A and S3B). Of relevance, gene and protein expression for the chemokine receptor Ccr9, which is critical for migration of thymus-seeding progenitors from the BM to the thymus (Schwarz et al., 2007), was suppressed in *Flt3*$^{ITD/ITD}$ LSKCD150$^-$48$^+$ MPPs (Figures 3D, S3C, and S3D). Moreover, DN1 cells showed large reductions in expression of *Notch1* and its targets (*Hes1* and *Hes5*; Figure S3E), which are critical for early T cell development. Although expression of some early lymphoid genes (*Il2ra*, *Il7r*, and *Gata3*) was maintained, myeloid genes (*Cebpa*, *Sfpi1*, *Csf1r*, *Csf2r*, and *Csf3r*) were highly upregulated in DN1 thymic progenitors (Figure S3E). In keeping with this myeloid bias, *Flt3*$^{ITD/ITD}$ DN1 progenitors showed low T cell potential in vitro (Figure 3E).

Previous studies demonstrated a reduction of mature B cells in *Flt3-ITD* mice (Lee et al., 2007; Li et al., 2008). We investigated whether this might reflect *Flt3-ITD*-induced perturbation at the earliest B cell commitment stages, and in support of this found a notable 11-fold expansion of Lin$^-$CD19$^-$CD24$^-$AA4.1$^+$CD43^{mid}B220$^+$ pre-pro-B cells in *Flt3*$^{ITD/ITD}$ mice (Figures 3F and 3G), whereas pro-B cells, the next stage in B cell development, were severely reduced (Figures 3H and S3F). Because pre-pro-B cells are known to sustain low-level myeloid potential (Rumfelt et al., 2006), we next investigated lymphoid and myeloid gene expression in *Flt3*$^{ITD/ITD}$ pre-pro-B cells. Key early lymphoid genes (*Cd79a*, *Il7r*, *sIgh*, *Ebf1*, *Pax5*, *Rag1*, and *Rag2*) were all suppressed (Figure 3I), whereas myeloid-affiliated genes (*Cebpa*, *Cebpb*, *Sfpi1*, *Csf1r*, and *Csf2r*) were upregulated in *Flt3*$^{ITD/ITD}$ pre-pro-B cells (Figure 3J). In agreement with this, *Flt3*$^{ITD/ITD}$ pre-pro-B cells had severely reduced B cell potential (Figure 3K). These findings demonstrate that Flt3-ITDs markedly impair the earliest stage of both T and B lymphopoiesis and upregulate myeloid gene expression in the earliest B and T lymphoid progenitors, in agreement with the notion that myeloid bias initiates in multipotent LMPPs.

Flt3-ITD-Induced Myeloid Bias Is Dependent on Upregulation of Pu1

To further explore the mechanistic basis of Flt3-ITD-induced myeloid bias of early lymphoid progenitors, we examined Pu1 protein expression using a Pu1-YFP reporter line. Whereas in wild-type (WT) mice Lin$^-$ cells showed a bimodal distribution between Pu1$^{low/-}$ and Pu1^{high} cells, almost all Lin$^-$ cells in *Flt3*$^{ITD/ITD}$ mice were Pu1^{high} (Figure 4A). *Flt3*$^{ITD/ITD}$ mice showed a modest increase in Pu1 expression in LSKCD150$^-$48$^+$ MPPs (Figure 4B) and markedly enhanced levels of Pu1-YFP in pre-pro-B cells (Figure 4C). In keeping with the observed increased expression of Pu1, gene set enrichment analysis (GSEA) demonstrated upregulation of Pu1 target genes (Steidl et al., 2006) in *Flt3-ITD* LSKCD150$^-$48$^+$ MPPs (Figure 4D). Furthermore, GSEA also demonstrated a similar upregulation of Pu1 target genes in *FLT3-ITD* mutated "LMPP-like" leukemia stem cells in human AML (Goardon et al., 2011) in comparison with FLT3-WT counterparts (Figure S4A).

Because transition from pre-pro-B cells to subsequent stages of B cell development is associated with downregulation of Pu1 expression (Figure S4B), we attempted to rescue the suppressed B cell phenotype in Flt3-ITD mice through generation of *Flt3*$^{ITD/ITD}$ Pu1$^{+/-}$ mice. Notably, whereas Pu1 haploinsufficiency did not increase the number of B cells or their progenitors on a WT background, it resulted in a 10.3-fold increase in B cells in *Flt3*$^{ITD/ITD}$ mice (Figure 4E). Furthermore, Pu1 haploinsufficiency led to a 2-fold reduction in the expanded pre-pro-B cell population in Flt3-ITD mice (Figure 4F) together with a 13.5-fold rescue of the suppression of pro-B cells (Figure 4G). Strikingly, in the presence of Pu1 haploinsufficiency, the expansion of MPPs was also restored to WT levels (Figure 4H) together with a significant amelioration of the myeloproliferative phenotype in *Flt3*$^{ITD/ITD}$ mice (Figure 4I).

Stat3 is aberrantly activated by Flt3-ITD signaling (Schmidt-Arras et al., 2009) and Pu1 is a direct target gene of Stat3 (Hegde et al., 2009). In line with this, *Flt3*$^{ITD/ITD}$ BM showed aberrant activation of STAT3 (Figure S4C), and MPPs and pre-pro-B cells showed significantly increased expression of Stat3 target genes (Figures 4J–4L). Collectively, these data suggest that Pu1 upregulation is a key mediator of the Flt3-ITD-induced myeloid bias and progenitor phenotype.

DISCUSSION

In the studies presented here, we explored whether and how GFR signaling might influence lineage specification in vivo. To

(E) Reduced MkE-affiliated gene expression in LSKCD48$^+$150$^-$ cells from *Flt3*$^{+/+}$, *Flt3*$^{ITD/+}$, and *Flt3*$^{ITD/ITD}$ mice relative to *Flt3*$^{+/+}$ LSK FLT3$^-$ cells; p values represent a comparison of *Flt3*$^{+/+}$LSK FLT3$^-$ cells versus LSKCD48$^+$150$^-$ *Flt3*$^{ITD/ITD}$ cells by unpaired t test (n = 6–8 replicates from 2–3 mice per genotype). Differences among *Flt3*$^{+/+}$, *Flt3*$^{ITD/+}$, and *Flt3*$^{ITD/ITD}$ MPPs were not significant.
(F) Single-cell Mk potential of *Flt3*$^{+/+}$and *Flt3*$^{ITD/ITD}$ LSKCD48$^+$150$^-$ MPPs in comparison with *Flt3*$^{+/+}$LSKCD48$^-$150$^+$ HSCs (n = 3 independent experiments).
(G) GSEA demonstrating upregulation of myeloid affiliated genes in *Flt3*$^{ITD/ITD}$ versus *Flt3*$^{+/+}$LSKCD48$^+$150$^-$ MPPs (n = 4 of each genotype).
(H) Single-cell GM potential of *Flt3*$^{+/+}$and *Flt3*$^{ITD/ITD}$ LSKCD48$^+$150$^-$ MPPs. Open bars show the frequency of clones formed, and closed bars show the frequency of highly proliferative clones (covering >50% of the well; n = 3 independent experiments).
(I) GSEA demonstrating downregulation of lymphoid transcriptional program in *Flt3*$^{ITD/ITD}$ versus *Flt3*$^{+/+}$ LSKCD48$^+$150$^-$ MPPs (n = 4 of each genotype).
(J) Expression of lymphoid-affiliated genes in LSKCD48$^+$150$^-$ MPPs from *Flt3*$^{+/+}$, *Flt3*$^{ITD/+}$, and *Flt3*$^{ITD/ITD}$ mice (n = 6–8 replicates from 2–3 mice per genotype); p values indicate comparisons of *Flt3*$^{+/+}$ versus *Flt3*$^{ITD/+}$ MPPs, and *Flt3*$^{+/+}$ versus *Flt3*$^{ITD/ITD}$ MPPs by unpaired t test ($p < 0.001$ for all analyses).
(K) B cell potential (B220$^+$CD19$^+$) of *Flt3*$^{+/+}$ versus *Flt3*$^{ITD/ITD}$ BM LSKCD48$^+$150$^-$ MPPs (10 cells/well). Data are mean (SEM) values of 2–3 experiments, with 9–12 replicate wells in each experiment.
Error bars represent SEM. See also Figure S2.

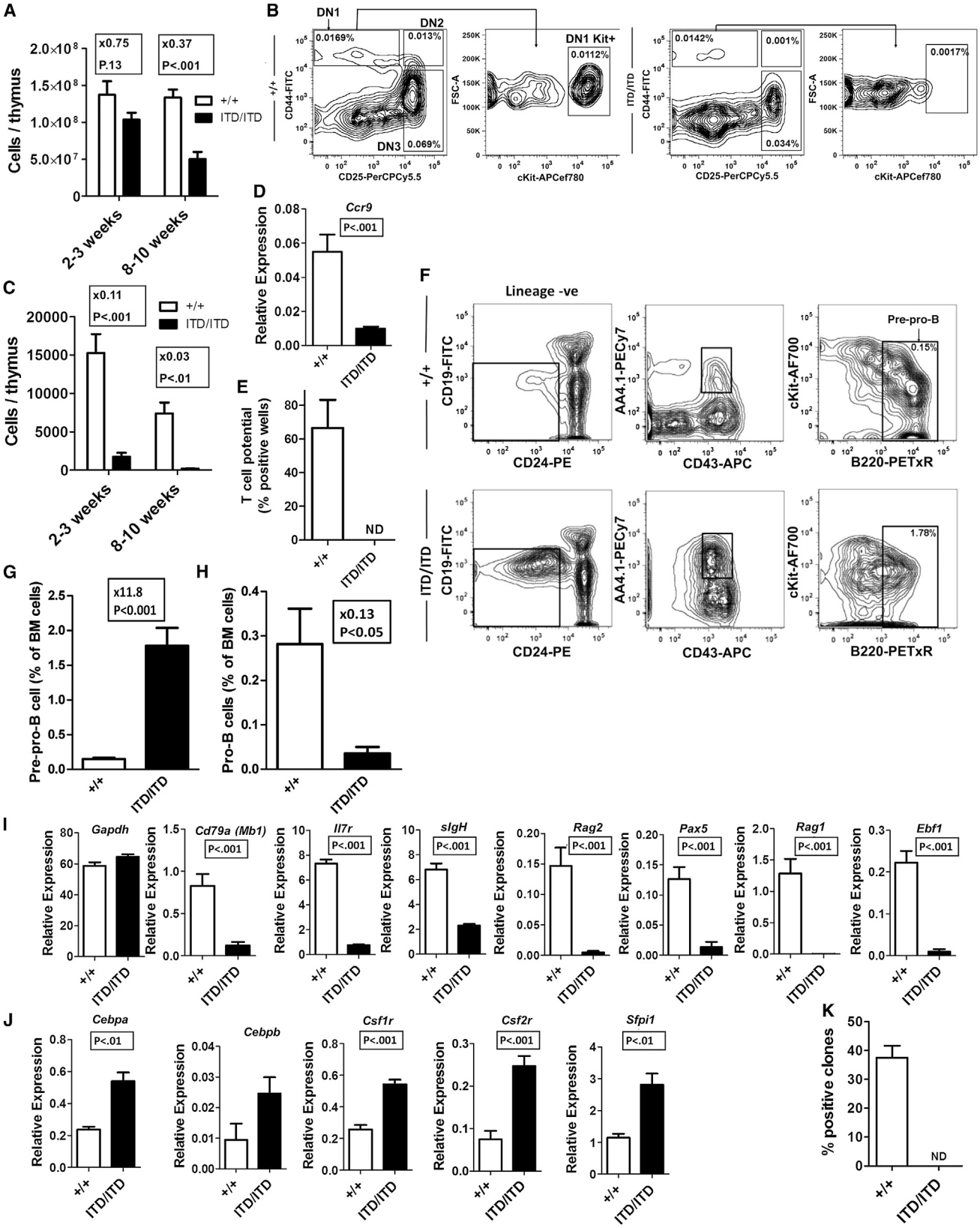

(legend on next page)

that end, we used a knockin model of *Flt3-ITD* to investigate whether oncogenic mutations that result in constitutive GFR signaling influence the lineage fate of MPPs in vivo.

In order to first establish the physiological relevance of Flt3-ITD as an AML-inducing mutation, we developed a mouse model in which *Flt3-ITD* was coexpressed with an inducible deletion of the DNA-binding domain of *Runx1* (Growney et al., 2005) in MPPs. Importantly, although Runx1 loss-of-function mutations are found in patients with both ALL and AML, only the latter is often found in association with FLT3-ITDs (Grossmann et al., 2011; Schnittger et al., 2011). Deletion of the DNA-binding domain of Runx1 during adult murine hematopoiesis results in mild myeloproliferation (Growney et al., 2005) or lymphoblastic leukemias/lymphomas (Jacob et al., 2010; Kundu et al., 2005; Putz et al., 2006). Here, we demonstrate that the combination of *Runx1* mutation with Flt3-ITDs results in aggressive leukemia with 100% penetrance and a uniform myeloid phenotype. In addition to demonstrating the functional relevance for FLT3-ITD-induced AML, this AML model has a number of important features. First, in contrast to many other mutation collaboration models, both mutations are targeted to the physiologically relevant endogenous genetic loci. Second, in isolation each mutation results in only a modest phenotype, but in combination a minor clone of deleted cells rapidly expands and becomes clonally dominant, paralleling somatic mutations during leukemogenesis. Third, the evolution of leukemia is rapid, supporting the notion that it occurs without the requirement for additional genetic events. Finally, the model recapitulates a particularly poor prognostic form of AML with a major unmet need for novel therapeutic approaches and thus provides a powerful model for future studies of the cellular and molecular mechanistic bases for collaboration of these mutations in AML.

The most primitive progenitor population that was expanded by Flt3-ITDs consisted of LMPP-like cells, demonstrating upregulation of the myeloid program, whereas the transcriptional expression of lymphoid-affiliated genes was markedly reduced in both heterozygous and homozygous Flt3-ITD mice. This myeloid transcriptional bias and suppression of lymphoid transcripts was also present during early B and T cell development and, importantly, was already present in Flt3-ITD FL MPPs, preceding the expansion of MPPs and development of a myeloproliferative phenotype, supporting the notion that it is a direct consequence of Flt3-ITD signaling in LMPPs. The severe suppression of the earliest thymic progenitors in *Flt3-ITD* mice and concomitant lack of Ccr9 upregulation in LMPPs, which have been implicated as key thymus-seeding progenitors (Luc et al., 2012), further suggests that thymic seeding might also be impaired by Flt3-ITDs. These findings demonstrate that the myeloid propensity of FLT3-ITDs results from FLT3-ITD introducing a myeloid bias in multipotent lymphomyeloid progenitors as well as in the earliest B and T lymphoid progenitors.

Pu1 is a dosage-sensitive regulator of myeloid-lymphoid cell-fate decisions that promotes myeloid differentiation when overexpressed (DeKoter and Singh, 2000). Using a Pu1-YFP reporter, we demonstrated that Flt3-ITDs upregulate Pu1 expression in MPPs and the earliest B lymphoid progenitors, paralleled by increased expression of Pu1 target genes in MPPs. Furthermore, we confirmed the relevance of these findings for human AML by demonstrating upregulation of Pu1 target genes in FLT3-ITD mutated LMPP-like human AML stem cells (Goardon et al., 2011). In agreement with a key mechanistic role for Pu1 overexpression, Flt3-ITD-induced suppression of B cell development, as well as the Flt3-ITD-associated progenitor phenotype, was partially rescued by Pu1 haploinsufficiency.

Constitutive Flt3-ITD signaling is distinct from WT Flt3 signaling due to abnormal anchoring of FLT3-ITD in the endoplasmic reticulum, with markedly reduced surface Flt3 expression resulting in aberrant Stat3 activation, as confirmed in our study (Schmidt-Arras et al., 2009). Because Pu1 is a direct target gene of Stat3 (Hegde et al., 2009) and Stat3 target genes were upregulated in *Flt3-ITD* LSKCD150^{-}48^{+} MPPs and pre-pro-B cells, this provides a putative direct link between aberrant constitutive Flt3-ITD signaling and Pu1 overexpression as a cause of aberrant myeloid bias.

Several lines of evidence indicate that FLT3-ITDs frequently arise early in the transformation process in MPPs (Levis et al., 2005) and as a driver mutation in the founding leukemic clone (Ding et al., 2012; Smith et al., 2012), and thus may influence the lineage of resulting leukemias. Together with our findings,

Figure 3. Early T and B Cell Progenitors Are Suppressed and Myeloid Biased in *Flt3*$^{ITD/ITD}$ Mice

(A) Thymic cellularity of *Flt3*$^{+/+}$ and *Flt3*$^{ITD/ITD}$ mice at 2–3 and 8–10 weeks (n = 7–10 mice of each genotype at each age).

(B) Representative DN staging of *Flt3*$^{+/+}$ and *Flt3*$^{ITD/ITD}$ thymocytes from 2-week-old mice; percentages are relative to total thymocytes.

(C) Progressive reduction of DN1Kit^{+} cells in *Flt3*$^{ITD/ITD}$ thymus.

(D) Expression (SEM) of *Ccr9* in LSKCD48^{+}150^{-} BM cells from 8- to 10-week-old *Flt3*$^{+/+}$ and *Flt3*$^{ITD/ITD}$ mice (n = 3–4 mice per genotype, 2–3 separately sorted replicates per mouse).

(E) T cell potential on OP9DL1 cells of DN1 cells (10/cells per well) from 2- to 3-week-old *Flt3*$^{+/+}$ and *Flt3*$^{ITD/ITD}$ mice (n = 2 mice per genotype, 12 replicate wells per mouse). ND, not detected.

(F) Representative staging of early B cell progenitors in *Flt3*$^{+/+}$ and *Flt3*$^{ITD/ITD}$ 2- to 3-week-old mice. pre-pro-B cells are identified as Lin^{-}B220^{+}CD19^{-}CD24^{-}AA4.1^{+}CD43^{mid}; percentage of total BM cells.

(G) Increased numbers of pre-pro-B cells in 2- to 3-week-old *Flt3*$^{ITD/ITD}$ mice (mean [SEM] values for 2- to 3-week-old mice, n = 8–10 of each genotype).

(H) Reduced numbers of pro-B cells (Lin^{-}B220^{+}CD43^{+}CD19^{+}CD24^{int}AA4.1^{+}) in *Flt3*$^{ITD/ITD}$ mice.

(I) Mean (SEM) expression of lymphoid-affiliated genes in pre-pro-B cells from 2- to 3-week-old mice (n = 2 mice per genotype, 3 separately sorted replicates per mouse).

(J) Mean (SEM) expression of myeloid-affiliated genes in pre-pro-B cells from *Flt3*$^{ITD/ITD}$ mice.

(K) In vitro B cell potential (B220^{+}CD19^{+} cells) of pre-pro-B cells from 2- to 3-week-old mice (n = 10 cells/well, 2 mice per genotype, 10 replicate wells per mouse). Error bars represent SEM. See also Figure S3.

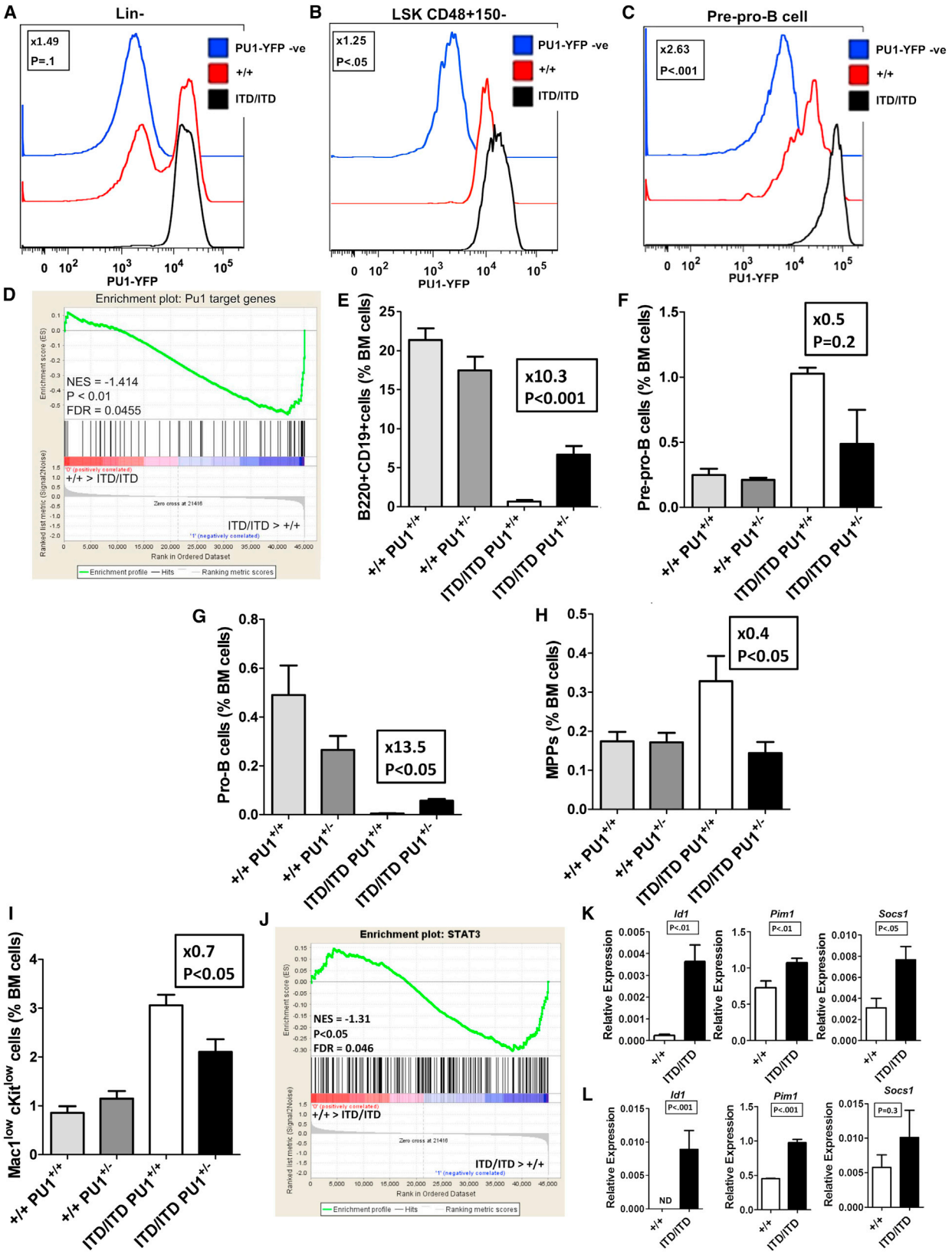

(legend on next page)

this is consistent with a model in which LMPPs, which normally express high levels of FLT3 (Adolfsson et al., 2005), acquire FLT3-ITD mutations that confer both a strong clonal advantage and a marked myeloid bias. This results in myeloid expansion and suppression of early lymphoid development, strongly supporting a fundamental role for FLT3-ITDs in promoting myeloid lineage leukemia development at the MPP level. Our study also further highlights LMPPs as a key target population in AML, as also supported by recent findings in human AML (Goardon et al., 2011). Transformation to an aggressive leukemia exclusively of a myeloid phenotype by introduction of Runx1 mutation demonstrates the functional relevance of this FLT3-ITD-induced myeloid bias and clonal dominance, providing insights into the process by which oncogenic mutations might determine the lineage fate of the resulting leukemias at the pre-commitment stage. Our findings are also of considerable relevance for normal hematopoiesis, as it remains disputed whether key cytokine receptor signaling pathways mediate critical in vivo functions in blood lineage development through purely permissive rather than instructive actions (Enver and Jacobsen, 2009). Thus, although Flt3-ITD elicits aberrant signaling, our findings clearly provide support for the notion that cytokine receptors are also capable of eliciting lineage-instructive signaling in MPPs in vivo.

EXPERIMENTAL PROCEDURES

Animals
All animals used were bred and maintained in accordance with regulations of the UK Home Office. Details regarding the mouse lines are provided in the Extended Experimental Procedures.

Patient Samples
BM samples from AML patients were obtained with informed consent and the approval of Oxford Ethics Committee B (protocols 06/Q1606/110 and 05/MRE07/74).

Fluorescence-Activated Cell Sorting
Details of the antibody staining panels and protocols are provided in the Extended Experimental Procedures. Antigens and antibodies used for identification of specific cell populations are shown in Tables S1 and S2.

Western Blotting
Cells were lysed in 1% NP40 buffer and analyzed by western blot as previously described (Pecquet et al., 2010) with antibodies against pStat3 (Cell Signaling) and beta-actin (Sigma).

In Vitro Evaluation of Lineage Potentials
Evaluation of megakaryocytic, GM, and lymphoid potentials was carried out as previously described (Månsson et al., 2007) and detailed in the Extended Experimental Procedures.

Gene Expression by Dynamic Arrays
Multiplex quantitative PCR was performed as previously described (Kharazi et al., 2011) and detailed in the Extended Experimental Procedures. Assays used for dynamic arrays are shown in Table S3.

Microarray Analysis
Analysis by Affymetrix Mouse Genome 430 2.0 Arrays was carried out at the Stanford Protein and Nucleic Acid Facility as described previously (Månsson et al., 2007) and in the Extended Experimental Procedures.

ACCESSION NUMBERS

The GEO accession number for the microarray data reported in this paper is GSE35805.

SUPPLEMENTAL INFORMATION

Supplemental Information includes Extended Experimental Procedures, four figures, and three tables and can be found with this article online at http://dx.doi.org/10.1016/j.celrep.2013.04.031.

LICENSING INFORMATION

ACKNOWLEDGMENTS

We thank Gary Gilliland for kindly providing Flt3-ITD knockin mice. A.M. and D.A. were funded by a Leukaemia and Lymphoma Research Senior Bennett Fellowship, S.K. was funded by the Pasteur Institute of Iran, and S.E.W.J. was funded through a Strategic Appointment and Programme grant from the

Figure 4. Involvement of PU1 Upregulation in the Myeloid Bias of *Flt3*$^{ITD/ITD}$ Mice

(A–C) Representative FACS analysis of PU1-YFP expression in lineage-negative (A), LSKCD48$^+$150$^-$ MPPs (B), and Lin$^-$CD19$^-$CD24$^-$AA4.1$^+$CD43^{mid}B220$^+$ pre-pro-B (C) cells in BM of 2- to 3-month-old *Flt3*$^{+/+}$ and *Flt3*$^{ITD/ITD}$ mice. Also shown is the mean fold difference in PU1-YFP expression for each population from six mice of each genotype.

(D) GSEA demonstrating upregulation of Pu1 target genes in LSKCD48$^+$150$^-$ MPPs from *Flt3*$^{ITD/ITD}$ versus *Flt3*$^{+/+}$ mice (n = 4 of each genotype).

(E) Percentage of B220$^+$CD19$^+$ in the BM of 6- to 8-week-old *Flt3*$^{+/+}$*Pu1*$^{+/+}$, *Flt3*$^{+/+}$*Pu1*$^{+/-}$, *Flt3*$^{ITD/ITD}$*Pu1*$^{+/+}$, and *Flt3*$^{ITD/ITD}$*Pu1*$^{+/-}$ mice (n = 8–11 mice of each genotype; fold difference and p value are for the difference between *Flt3*$^{ITD/ITD}$*Pu1*$^{+/+}$ and *Flt3*$^{ITD/ITD}$*Pu1*$^{+/-}$ mice).

(F) Percentage of pre-pro-B cells in the BM of 6- to 8-week-old *Flt3*$^{+/+}$*Pu1*$^{+/+}$, *Flt3*$^{+/+}$*Pu1*$^{+/-}$, *Flt3*$^{ITD/ITD}$*Pu1*$^{+/+}$ and *Flt3*$^{ITD/ITD}$*Pu1*$^{+/-}$ mice (n = 3 mice of each genotype).

(G) Percentage of pro-B cells in the BM of 6- to 8-week-old *Flt3*$^{+/+}$*Pu1*$^{+/+}$, *Flt3*$^{+/+}$*Pu1*$^{+/-}$, *Flt3*$^{ITD/ITD}$*Pu1*$^{+/+}$ and *Flt3*$^{ITD/ITD}$*Pu1*$^{+/-}$ mice (n = 3 mice of each genotype).

(H) Percentage of LSKCD48$^+$150$^-$ MPPs in the BM of 6- to 8-week-old *Flt3*$^{+/+}$*Pu1*$^{+/+}$, *Flt3*$^{+/+}$*Pu1*$^{+/-}$, *Flt3*$^{ITD/ITD}$*Pu1*$^{+/+}$ and *Flt3*$^{ITD/ITD}$*Pu1*$^{+/-}$ mice (n = 7–9 mice of each genotype).

(I) Percentage of Mac1^{low}cKit^{low} myeloid precursor cells in the BM of 6- to 8-week-old *Flt3*$^{+/+}$*Pu1*$^{+/+}$, *Flt3*$^{+/+}$*Pu1*$^{+/-}$, *Flt3*$^{ITD/ITD}$*Pu1*$^{+/+}$ and *Flt3*$^{ITD/ITD}$*Pu1*$^{+/-}$ mice (n = 7–9 mice of each genotype).

(J) GSEA demonstrating upregulation of STAT3 target genes in *Flt3*$^{ITD/ITD}$ versus *Flt3*$^{+/+}$ LSKCD48$^+$150$^-$ MPPs (n = 4 mice of each genotype).

(K and L) Expression of Stat3 target genes in *Flt3*$^{+/+}$ and *Flt3*$^{ITD/ITD}$ LSKCD48$^+$150$^-$ MPPs (K) and pre-pro-B cells (L) (n = 2–4 mice of each genotype, 2–3 replicates per mouse). ND, not detected.

Error bars represent SEM. See also Figure S4.

Medical Research Council (UK) and a Hemato-Linné grant (Swedish Research Council Linnaeus). A.M., P.V., and S.E.J. were supported by the National Institute for Health Research (NIHR) Oxford Biomedical Research Centre based at Oxford University Hospitals NHS Trust, and by the NCRN MDSBio sample collection study. The views expressed are those of the author(s) and not necessarily those of the NHS, the NIHR, or the Department of Health. A.M. designed, performed, and analyzed experiments and wrote the manuscript. Support to S.N.C. from Fondation contre le cancer, Salus Sanguinis, Action de Recherche Concertée and Interuniversity Attraction Poles Programs and Fonds de la Recherche Scientifique, Belgium and Ludwig Institute for Cancer Research is acknowledged. S.K. performed and analyzed experiments. D.A. provided technical assistance. I.M. and N.G. analyzed microarray data. S. Loughran, M.L., P.W., O.C., S. Luc, N.B.V., H.F., and S.A.C. were involved in FACS analysis/sorting. C.P. performed western blotting. E.S., P.V., S.C., and C.N. provided input on experimental design and analysis. S.E.W.J. conceived and supervised the project, designed and analyzed experiments, and wrote the manuscript.

Received: January 12, 2012
Revised: March 12, 2013
Accepted: April 29, 2013
Published: May 30, 2013

REFERENCES

Adolfsson, J., Månsson, R., Buza-Vidas, N., Hultquist, A., Liuba, K., Jensen, C.T., Bryder, D., Yang, L., Borge, O.J., Thoren, L.A., et al. (2005). Identification of Flt3+ lympho-myeloid stem cells lacking erythro-megakaryocytic potential a revised road map for adult blood lineage commitment. Cell *121*, 295–306.

Chu, S.H., Heiser, D., Li, L., Kaplan, I., Collector, M., Huso, D., Sharkis, S.J., Civin, C., and Small, D. (2012). FLT3-ITD knockin impairs hematopoietic stem cell quiescence/homeostasis, leading to myeloproliferative neoplasm. Cell Stem Cell *11*, 346–358.

Croce, C.M. (2008). Oncogenes and cancer. N. Engl. J. Med. *358*, 502–511.

DeKoter, R.P., and Singh, H. (2000). Regulation of B lymphocyte and macrophage development by graded expression of PU.1. Science *288*, 1439–1441.

Ding, L., Ley, T.J., Larson, D.E., Miller, C.A., Koboldt, D.C., Welch, J.S., Ritchey, J.K., Young, M.A., Lamprecht, T., McLellan, M.D., et al. (2012). Clonal evolution in relapsed acute myeloid leukaemia revealed by whole-genome sequencing. Nature *481*, 506–510.

Enver, T., and Jacobsen, S.E. (2009). Developmental biology: Instructions writ in blood. Nature *461*, 183–184.

Gale, R.E., Green, C., Allen, C., Mead, A.J., Burnett, A.K., Hills, R.K., and Linch, D.C.; Medical Research Council Adult Leukaemia Working Party. (2008). The impact of FLT3 internal tandem duplication mutant level, number, size, and interaction with NPM1 mutations in a large cohort of young adult patients with acute myeloid leukemia. Blood *111*, 2776–2784.

Goardon, N., Marchi, E., Atzberger, A., Quek, L., Schuh, A., Soneji, S., Woll, P., Mead, A., Alford, K.A., Rout, R., et al. (2011). Coexistence of LMPP-like and GMP-like leukemia stem cells in acute myeloid leukemia. Cancer Cell *19*, 138–152.

Grossmann, V., Kern, W., Harbich, S., Alpermann, T., Jeromin, S., Schnittger, S., Haferlach, C., Haferlach, T., and Kohlmann, A. (2011). Prognostic relevance of RUNX1 mutations in T-cell acute lymphoblastic leukemia. Haematologica *96*, 1874–1877.

Growney, J.D., Shigematsu, H., Li, Z., Lee, B.H., Adelsperger, J., Rowan, R., Curley, D.P., Kutok, J.L., Akashi, K., Williams, I.R., et al. (2005). Loss of Runx1 perturbs adult hematopoiesis and is associated with a myeloproliferative phenotype. Blood *106*, 494–504.

Hegde, S., Ni, S., He, S., Yoon, D., Feng, G.S., Watowich, S.S., Paulson, R.F., and Hankey, P.A. (2009). Stat3 promotes the development of erythroleukemia by inducing Pu.1 expression and inhibiting erythroid differentiation. Oncogene *28*, 3349–3359.

Jacob, B., Osato, M., Yamashita, N., Wang, C.Q., Taniuchi, I., Littman, D.R., Asou, N., and Ito, Y. (2010). Stem cell exhaustion due to Runx1 deficiency is prevented by Evi5 activation in leukemogenesis. Blood *115*, 1610–1620.

Jan, M., Snyder, T.M., Corces-Zimmerman, M.R., Vyas, P., Weissman, I.L., Quake, S.R., and Majeti, R. (2012). Clonal evolution of preleukemic hematopoietic stem cells precedes human acute myeloid leukemia. Sci. Transl. Med. *4*, 149ra118.

Kharazi, S., Mead, A.J., Mansour, A., Hultquist, A., Böiers, C., Luc, S., Buza-Vidas, N., Ma, Z., Ferry, H., Atkinson, D., et al. (2011). Impact of gene dosage, loss of wild-type allele, and FLT3 ligand on Flt3-ITD-induced myeloproliferation. Blood *118*, 3613–3621.

Kiel, M.J., Yilmaz, O.H., Iwashita, T., Yilmaz, O.H., Terhorst, C., and Morrison, S.J. (2005). SLAM family receptors distinguish hematopoietic stem and progenitor cells and reveal endothelial niches for stem cells. Cell *121*, 1109–1121.

Kundu, M., Compton, S., Garrett-Beal, L., Stacy, T., Starost, M.F., Eckhaus, M., Speck, N.A., and Liu, P.P. (2005). Runx1 deficiency predisposes mice to T-lymphoblastic lymphoma. Blood *106*, 3621–3624.

Lee, B.H., Tothova, Z., Levine, R.L., Anderson, K., Buza-Vidas, N., Cullen, D.E., McDowell, E.P., Adelsperger, J., Fröhling, S., Huntly, B.J., et al. (2007). FLT3 mutations confer enhanced proliferation and survival properties to multipotent progenitors in a murine model of chronic myelomonocytic leukemia. Cancer Cell *12*, 367–380.

Leow, S., Kham, S.K., Ariffin, H., Quah, T.C., and Yeoh, A.E. (2011). FLT3 mutation and expression did not adversely affect clinical outcome of childhood acute leukaemia—a study of 531 Southeast Asian children by the Ma-Spore study group. Hematol. Oncol. *29*, 211–219.

Levis, M., Murphy, K.M., Pham, R., Kim, K.T., Stine, A., Li, L., McNiece, I., Smith, B.D., and Small, D. (2005). Internal tandem duplications of the FLT3 gene are present in leukemia stem cells. Blood *106*, 673–680.

Li, L., Piloto, O., Nguyen, H.B., Greenberg, K., Takamiya, K., Racke, F., Huso, D., and Small, D. (2008). Knock-in of an internal tandem duplication mutation into murine FLT3 confers myeloproliferative disease in a mouse model. Blood *111*, 3849–3858.

Luc, S., Luis, T.C., Boukarabila, H., Macaulay, I.C., Buza-Vidas, N., Bouriez-Jones, T., Lutteropp, M., Woll, P.S., Loughran, S.J., Mead, A.J., et al. (2012). The earliest thymic T cell progenitors sustain B cell and myeloid lineage potential. Nat. Immunol. *13*, 412–419.

Månsson, R., Hultquist, A., Luc, S., Yang, L., Anderson, K., Kharazi, S., Al-Hashmi, S., Liuba, K., Thorén, L., Adolfsson, J., et al. (2007). Molecular evidence for hierarchical transcriptional lineage priming in fetal and adult stem cells and multipotent progenitors. Immunity *26*, 407–419.

Pecquet, C., Staerk, J., Chaligné, R., Goss, V., Lee, K.A., Zhang, X., Rush, J., Van Hees, J., Poirel, H.A., Scheiff, J.M., et al. (2010). Induction of myeloproliferative disorder and myelofibrosis by thrombopoietin receptor W515 mutants is mediated by cytosolic tyrosine 112 of the receptor. Blood *115*, 1037–1048.

Putz, G., Rosner, A., Nuesslein, I., Schmitz, N., and Buchholz, F. (2006). AML1 deletion in adult mice causes splenomegaly and lymphomas. Oncogene *25*, 929–939.

Rieger, M.A., Hoppe, P.S., Smejkal, B.M., Eitelhuber, A.C., and Schroeder, T. (2009). Hematopoietic cytokines can instruct lineage choice. Science *325*, 217–218.

Rumfelt, L.L., Zhou, Y., Rowley, B.M., Shinton, S.A., and Hardy, R.R. (2006). Lineage specification and plasticity in CD19- early B cell precursors. J. Exp. Med. *203*, 675–687.

Schmidt-Arras, D., Böhmer, S.A., Koch, S., Müller, J.P., Blei, L., Cornils, H., Bauer, R., Korasikha, S., Thiede, C., and Böhmer, F.D. (2009). Anchoring of FLT3 in the endoplasmic reticulum alters signaling quality. Blood *113*, 3568–3576.

Schnittger, S., Dicker, F., Kern, W., Wendland, N., Sundermann, J., Alpermann, T., Haferlach, C., and Haferlach, T. (2011). RUNX1 mutations are

frequent in de novo AML with noncomplex karyotype and confer an unfavorable prognosis. Blood *117*, 2348–2357.

Schwarz, B.A., Sambandam, A., Maillard, I., Harman, B.C., Love, P.E., and Bhandoola, A. (2007). Selective thymus settling regulated by cytokine and chemokine receptors. J. Immunol. *178*, 2008–2017.

Sitnicka, E., Bryder, D., Theilgaard-Mönch, K., Buza-Vidas, N., Adolfsson, J., and Jacobsen, S.E. (2002). Key role of flt3 ligand in regulation of the common lymphoid progenitor but not in maintenance of the hematopoietic stem cell pool. Immunity *17*, 463–472.

Smith, C.C., Wang, Q., Chin, C.S., Salerno, S., Damon, L.E., Levis, M.J., Perl, A.E., Travers, K.J., Wang, S., Hunt, J.P., et al. (2012). Validation of ITD mutations in FLT3 as a therapeutic target in human acute myeloid leukaemia. Nature *485*, 260–263.

Steidl, U., Rosenbauer, F., Verhaak, R.G., Gu, X., Ebralidze, A., Otu, H.H., Klippel, S., Steidl, C., Bruns, I., Costa, D.B., et al. (2006). Essential role of Jun family transcription factors in PU.1 knockdown-induced leukemic stem cells. Nat. Genet. *38*, 1269–1277.

Stirewalt, D.L., and Radich, J.P. (2003). The role of FLT3 in haematopoietic malignancies. Nat. Rev. Cancer *3*, 650–665.

Cell PRESS
Open ACCESS

EXTENDED EXPERIMENTAL PROCEDURES

Quantification of Hematologic Indices

Hemoglobin, WBC, and platelet count per milliliter of blood were quantified on a Sysmex® KX-21N 3-part differential hematology analyzer.

Animals

Flt3-ITD knockin mice on C57BL/6 background have been previously described (Kharazi et al., 2011; Lee et al., 2007). Homozygous (*Flt3*$^{ITD/ITD}$) and heterozygous (*Flt3*$^{ITD/+}$) *Flt3-ITD* mice were studied as specified. *Runx1*$^{fl/fl}$ mice have been previously described (Grundler et al., 2005) and were on a 129S1 x CBA background. *VavCre* mice have been previously described (de Boer et al., 2003) and were on a C57BL/6 background. *Mx1-Cre* mice were on C57BL/6 background and have been previously described (Kühn et al., 1995). Mice carrying a germline deletion of *Pu1* (*Pu1*$^{+/-}$) were derived by crossing a previously reported *Pu1*$^{fl/+}$ line (Iwasaki et al., 2005) on a C57BL/6 × 129S1 x CBA background with a constitutive CMV-Cre recombinase, on a C57BL/6 background. Pu1-YFP mice on a C57BL/6 background have been previously described (Kirstetter et al., 2006). Mice were analyzed with littermate controls of the appropriate genotype when available.

Flow Cytometry Analysis and FACS Purification

Antibodies and viability dyes used for flow cytometry analysis are shown in Table S1. Combinations of antibodies used for identification and purification of indicated populations are shown in Table S2.

All antibodies were used at predetermined (titrated) optimized concentrations. Cell acquisition and analysis were performed on a 4-laser LSRII (Becton Dickinson, San Jose, CA) using FlowJo software (TreeStar, Ashland, OR). Cell sorting was done on a BD FACSAriaII cell sorter (BD Biosciences). Cells used in cell sorting experiments were either un-enriched or enriched for CD117 with MACS cell separation (Miltenyi Biotec) followed by Fc-block incubation and staining with anti-mouse antibodies. Fluorescence minus-one controls as well as negative populations were used as gate-setting controls. Gates were set using a combination of fluorescence minus one controls and also populations that are known to be negative for the antigen. For example, LSKCD150^{+}CD48^{-} cells, which are known to not express Flt3, were used to set the gate for surface Flt3 expression on LSKCD150^{-}CD48^{+} cells.

Microarray Analysis

Global gene expression analysis was performed on LSKCD150^{-}CD48^{+} cells from *Flt3*$^{+/+}$ and *Flt3*$^{ITD/ITD}$ (4 mice of each genotype) as previously reported (Luc et al., 2012). Two thousand cells were sorted directly into Trizol (Invitrogen) and the RNA extraction carried out as per manufacturer's instructions and previously as described (Luc et al., 2012). Using the same total amount of input RNA, samples were amplified using the NuGEN kit WT-Ovation Pico RNA Amplifications System followed by the WT Ovation cDNA Biotin Module V2 for cDNA labeling (NuGEN) and fragmentation and finally hybridized to Affymetrix Mouse Genome 430 2.0 Arrays using standard protocols (Affymetrix) at the Stanford Protein and Nucleic Acid facility. These data will be available through GEO accession number GSE35805 (http://www.ncbi.nlm.nih.gov/geo/query/acc.cgi?token=dfcvjocouaoccds&acc=GSE35805).

Microarray data were normalized using the Robust Multi-array Averages (RMA)(Irizarry et al., 2003) method in Biocondcutor/R and analyzed using gene set enrichment analysis (GSEA) (Subramanian et al., 2005). Erythroid, myeloid (Chambers et al., 2007), Pu1 (Steidl et al., 2006), and STAT3 (Alvarez et al., 2005) target gene lists have been previously described. A signature for early B cell commitment was generated using data from the Immunological Genome Project (Heng et al., 2008) (http://www.immgen.org) by comparing the gene expression profile of long term reconstituting stem cells with that of pre-pro-B cells using the limma package (Smyth, 2004) in R; genes which were greater than 2-fold upregulated (limma B statistic > 3) were used for the B cell commitment signature. GSEA analysis of LMPP-like human AML stem cells, stratified according to the presence of *FLT3-ITD* mutation, was carried out using previously described data set (Goardon et al., 2011), using human equivalents of the above murine Pu1 target genes (Steidl et al., 2006).

Multiplex Quantitative Real-Time PCR Analysis

Multiplex quantitative PCR was performed as previously described (Kharazi et al., 2011). For each cell population, two to four biological replicates (different mice) were prepared, and two to three separately sorted cell samples from each mouse were cell sorted and analyzed. For LSKCD150^{-}CD48^{+} cells, LSKFlt3^{-} cells, and pre-pro-B cells, 100 cells per replicate were analyzed. For DN1 cells, 20 cells per replicate were analyzed as cell numbers of this population were highly limited in *Flt3*$^{ITD/ITD}$ mice. Details of the TaqMan assays used are shown in Table S3.

For cDNA synthesis and preamplification of target genes CellsDirect One-Step qRT-PCR kit (Invitrogen) was used. Cells were sorted directly into PCR plates or 0.2 ml PCR tubes containing 2.5 μl gene specific 0.2x TaqMan gene expression assays (Applied Biosystems), 5 μl of CellsDirect 2x Reaction mix (Invitrogen), 1.2 μl CellsDirect RT/Taq mix, 1.2 μl TE buffer and 0.1 μl SUPERase-In RNase Inhibitor (Ambion). Conditions for reverse transcription and target gene amplification were: 15 min at 50°C; 2 min at 95°C; 22 cycles of 95°C for 15 s and 60°C for 4 min. Preamplified products were diluted 1:5 in TE buffer and analyzed on Dynamic Array

(Fluidigm) using the following PCR cycling condition: 95°C for 10 min; 40 cycles of 95°C for 15 s and 60°C for 60 s. Data was analyzed using the ΔCt method; results were normalized to *Hprt* expression and expressed as mean expression level relative to *Hprt*.

In Vitro Assays for Megakaryocyte, GM, and Lymphoid Potentials

Evaluation of megakaryocytic and GM potentials was carried out as previously described (Luc et al., 2008). For evaluation of megakaryocytic potential, 150 cells were sorted into 3 ml of X-vivo 15 (Lonza) supplemented with 0.5% detoxified Bovine Serum Albumin (BSA; StemCell Technologies Inc), 10% fetal calf serum (FCS), 2-mercaptoethanol (2-ME; 10^{-4} M; Sigma-Aldrich Co), 1% penicillin/streptomycin (PAA) and 50 ng/mL murine stem cell factor (mSCF; PeproTech, Rocky Hill, NJ), 50 ng/mL human fms-like tyrosine kinase 3 ligand (hFL; Immunex, Seattle, WA), 50 ng/mL human thrombopoietin (hTHPO; PeptroTech), 5 U/mL human erythropoietin (hEPO; Boehringer Mannheim, Mannheim, Germany) and 20 ng/mL murine interleukin 3 (mIL-3; PeproTech). For evaluation of GM potential, cells were sorted into media as above but with the following cytokines: mSCF, hFL, hTHPO, hG-CSF (Neopogen, Amgen, Thousand Oaks, CA) (all 25 ng/mL), mGM-CSF (Immunex, Seattle, WA) and mIL-3 (both 20 ng/mL). The cell suspension was thoroughly mixed and 20 μl was pipetted into each well of two 60-well plates per replicate (Nunc Minitrays catalog number: 163118, Nunc A/S, Roskilde, Denmark). Wells were scored for clonal growth and/or frequency of wells with megakaryocytes with an inverted light microscope after 8 days of culture. The reliability of this approach to score cultures for megakaryocytic potential has been validated by morphological validation of Giemsa stained cytospins of the cultures (Månsson et al., 2007). Percentage of cloning efficiency was calculated according to the Poisson distribution which predicts that 63% of wells should contain 1 or more cells following manual plating (76 of 120 wells).

B cell and T cell potential was evaluated by sorting 10 MPPs, DN1 or pre-pro-B cells onto approximately 80% confluent monolayers of OP9 (B cell potential) and OP9DL1 (T cell potential) stromal cells, as previously described (Adolfsson et al., 2005; Luc et al., 2012). Clones were identified and picked at 3 to 4 weeks (depending on clonal size), and subsequently analyzed by FACS for the presence of B cell (defined as $B220^{+}CD19^{+}$) or T cell (CD4/8 double positive) committed progeny.

Statistical Analysis

The statistical significance of differences between samples was determined using the 2-tailed t test.

SUPPLEMENTAL REFERENCES

Alvarez, J.V., Febbo, P.G., Ramaswamy, S., Loda, M., Richardson, A., and Frank, D.A. (2005). Identification of a genetic signature of activated signal transducer and activator of transcription 3 in human tumors. Cancer Res. *65*, 5054–5062.

Chambers, S.M., Boles, N.C., Lin, K.Y., Tierney, M.P., Bowman, T.V., Bradfute, S.B., Chen, A.J., Merchant, A.A., Sirin, O., Weksberg, D.C., et al. (2007). Hematopoietic fingerprints: an expression database of stem cells and their progeny. Cell Stem Cell *1*, 578–591.

de Boer, J., Williams, A., Skavdis, G., Harker, N., Coles, M., Tolaini, M., Norton, T., Williams, K., Roderick, K., Potocnik, A.J., and Kioussis, D. (2003). Transgenic mice with hematopoietic and lymphoid specific expression of Cre. Eur. J. Immunol. *33*, 314–325.

Grundler, R., Miething, C., Thiede, C., Peschel, C., and Duyster, J. (2005). FLT3-ITD and tyrosine kinase domain mutants induce 2 distinct phenotypes in a murine bone marrow transplantation model. Blood *105*, 4792–4799.

Heng, T.S., and Painter, M.W.; Immunological Genome Project Consortium. (2008). The Immunological Genome Project: networks of gene expression in immune cells. Nat. Immunol. *9*, 1091–1094.

Irizarry, R.A., Bolstad, B.M., Collin, F., Cope, L.M., Hobbs, B., and Speed, T.P. (2003). Summaries of Affymetrix GeneChip probe level data. Nucleic Acids Res. *31*, e15.

Iwasaki, H., Somoza, C., Shigematsu, H., Duprez, E.A., Iwasaki-Arai, J., Mizuno, S., Arinobu, Y., Geary, K., Zhang, P., Dayaram, T., et al. (2005). Distinctive and indispensable roles of PU.1 in maintenance of hematopoietic stem cells and their differentiation. Blood *106*, 1590–1600.

Kirstetter, P., Anderson, K., Porse, B.T., Jacobsen, S.E., and Nerlov, C. (2006). Activation of the canonical Wnt pathway leads to loss of hematopoietic stem cell repopulation and multilineage differentiation block. Nat. Immunol. *7*, 1048–1056.

Kühn, R., Schwenk, F., Aguet, M., and Rajewsky, K. (1995). Inducible gene targeting in mice. Science *269*, 1427–1429.

Luc, S., Anderson, K., Kharazi, S., Buza-Vidas, N., Böiers, C., Jensen, C.T., Ma, Z., Wittmann, L., and Jacobsen, S.E. (2008). Down-regulation of Mpl marks the transition to lymphoid-primed multipotent progenitors with gradual loss of granulocyte-monocyte potential. Blood *111*, 3424–3434.

Smyth, G.K. (2004). Linear models and empirical Bayes methods for assessing differential expression in microarray experiments. Stat. Appl. Genet. Mol. Biol. *3*, Article3.

Subramanian, A., Tamayo, P., Mootha, V.K., Mukherjee, S., Ebert, B.L., Gillette, M.A., Paulovich, A., Pomeroy, S.L., Golub, T.R., Lander, E.S., and Mesirov, J.P. (2005). Gene set enrichment analysis: a knowledge-based approach for interpreting genome-wide expression profiles. Proc. Natl. Acad. Sci. USA *102*, 15545–15550.

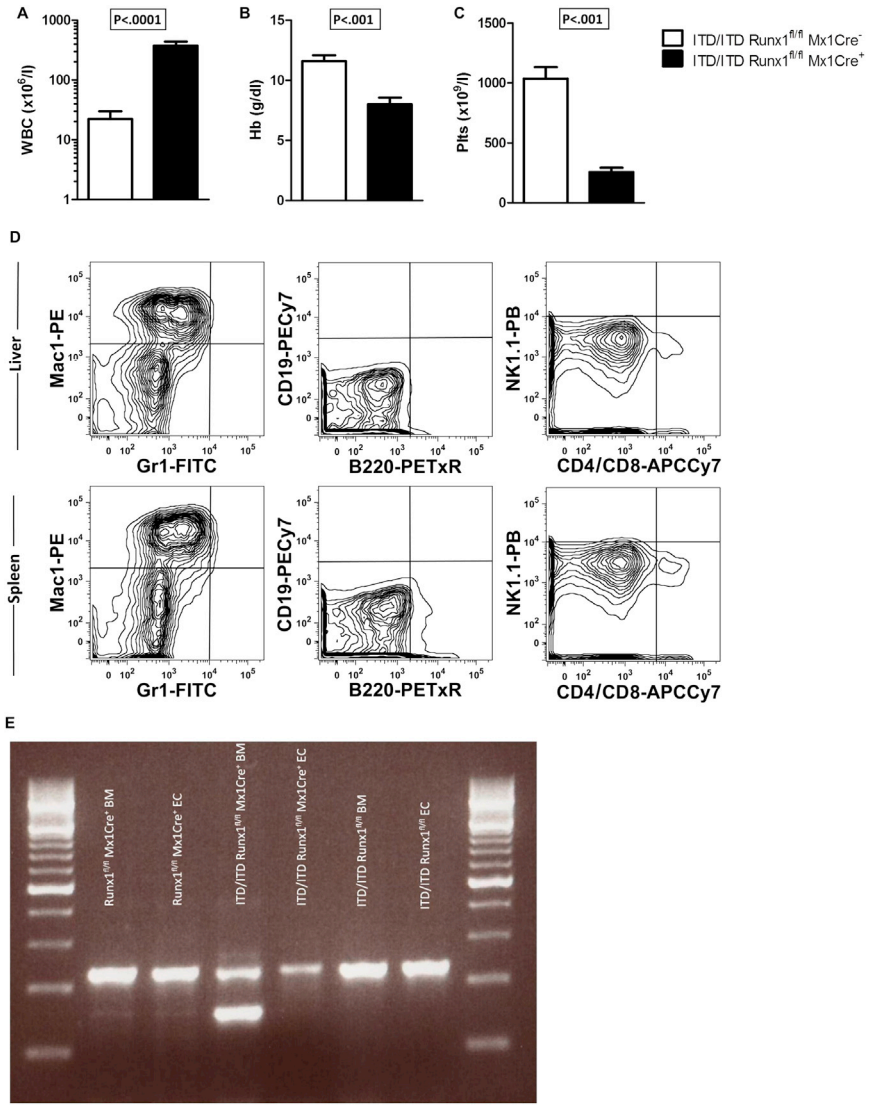

Figure S1. Mutation of *Runx1* in *Flt3*$^{ITD/ITD}$ Mice Results in High-Penetrance Aggressive Myeloid Leukemia, Related to Figure 1

(A–C) Hematologic indices in *Flt3*$^{ITD/ITD}$*Runx1*$^{fl/fl}$*Mx1Cre*$^{+}$ leukemic mice demonstrating a marked increase in white blood cell count (WBC) (A), anemia (B), and thrombocytopenia (C) compared with *Flt3*$^{ITD/ITD}$*Runx1*$^{fl/fl}$*Mx1Cre*$^{-}$ controls. Mean (SEM) values from 6-14 mice from 5-11 independent experiments. Hematologic indices were measured using a Sysmex® automated analyzer.

(D) Representative FACS analysis of infiltrated livers and spleens from *Flt3*$^{ITD/ITD}$*Runx1*$^{fl/fl}$*Mx1Cre*$^{+}$ leukemic mice showing lineage surface markers typical of myeloid leukemic cells (results representative of 3 [liver] and 11 [spleen] further analyzed cases).

(E) Recombination at the *Runx1* locus without poly I:C induction in *Flt3*$^{ITD/ITD}$*Runx1*$^{fl/fl}$*Mx1Cre*$^{+}$ leukemic BM. Representative PCR analysis of *Runx1*$^{fl/fl}$ recombination in paired BM and earclip (EC) DNA from *Flt3*$^{ITD/ITD}$*Runx1*$^{fl/fl}$*Mx1Cre*$^{+}$ leukemic and *Flt3*$^{ITD/ITD}$*Runx1*$^{fl/fl}$*Mx1Cre*$^{-}$ and *Flt3*$^{+/+}$*Runx1*$^{fl/fl}$*Mx1Cre*$^{+}$ controls, all without polyI:C induction. The upper band represents non-deleted *Runx1* allele and the lower band indicates deleted *Runx1* alleles. Results are representative of 3 further analyzed leukemic samples. Error bars represent SEM.

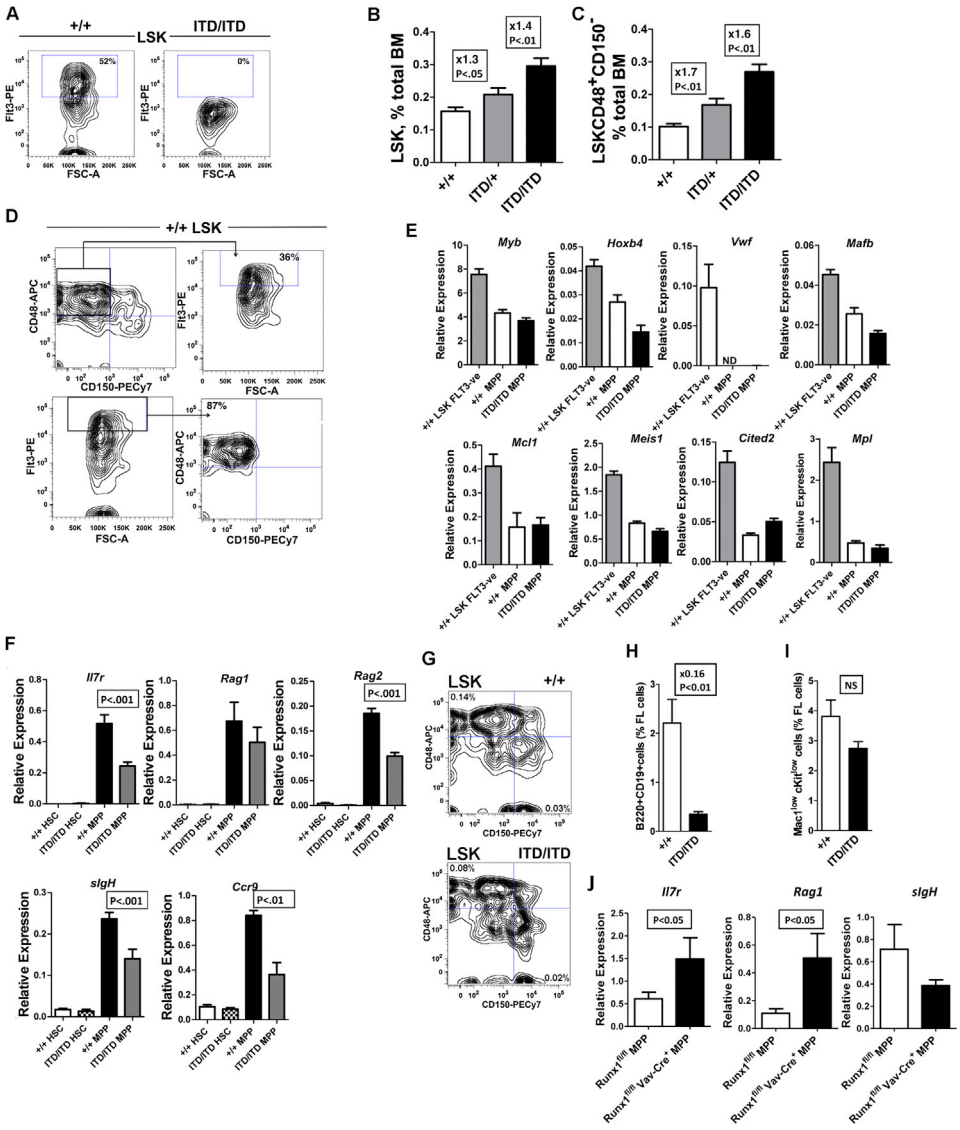

Figure S2. Flt3-ITDs Expand Myeloid-Biased LMPPs, Related to Figure 2

(A) Lack of cell surface Flt3 expression in *Flt3*$^{ITD/ITD}$ mice; representative FACS analysis of surface Flt3 expression in LSK cells from *Flt3*$^{+/+}$ and *Flt3*$^{ITD/ITD}$ mice. Percentages in the graph represent mean frequency of Flt3-positive cells in the LSK compartment of *Flt3*$^{+/+}$ (n = 27) and *Flt3*$^{ITD/ITD}$ (n = 23) mice.

(B) *Flt3*$^{ITD/+}$ mice show an intermediate expansion of LSK cells relative to *Flt3*$^{+/+}$ and *Flt3*$^{ITD/ITD}$ mice (*Flt3*$^{+/+}$ n = 27; *Flt3*$^{ITD/+}$ n = 13; and *Flt3*$^{ITD/ITD}$ n = 23).

(C) *Flt3*$^{ITD/+}$ mice show an expansion of LSKCD48^{+}CD150^{-} MPPs intermediate between *Flt3*$^{+/+}$ and *Flt3*$^{ITD/ITD}$ mice (*Flt3*$^{+/+}$ n = 27; *Flt3*$^{ITD/+}$ n = 13; and *Flt3*$^{ITD/ITD}$ n = 23).

(D) LMPPs reside in the LSKCD150^{-}48^{+} compartment; representative FACS analysis of CD48 and CD150 expression in relation to high-level Flt3 expressing LMPPs within the LSK compartment. High-level Flt3 expression was defined as the highest 20% of Flt3 staining cells in *Flt3*$^{+/+}$ LSK cells. Percentages in the graph represent mean frequency of indicated cells relative to parental gate from *Flt3*$^{+/+}$ (n = 17) mice.

(E) HSC associated gene expression is not upregulated in the LSKCD150^{-}48^{+} compartment in *Flt3*$^{ITD/ITD}$ mice. Mean (SEM) HSC affiliated gene expression in indicated cell populations from *Flt3*$^{+/+}$ and *Flt3*$^{ITD/ITD}$ mice. P-values are shown if < 0.05 (not reached for any comparison of *Flt3*$^{+/+}$ and *Flt3*$^{ITD/ITD}$ MPPs); ND indicates not detected.

(F) Expression of lymphoid affiliated genes in E15 FL LSKCD150^{+}CD48^{-} HSCs and LSKCD150^{-}CD48^{+} MPPs from *Flt3*$^{+/+}$ and *Flt3*$^{ITD/ITD}$ mice (n = 9 replicates from 3 mice per genotype). P values less than 0.05 are shown for comparison of *Flt3*$^{+/+}$ and *Flt3*$^{ITD/ITD}$ MPPs.

(G) LSKCD150^{-}48^{+} MPPs are not expanded in the fetal liver (FL) of *Flt3*$^{ITD/ITD}$ mice; representative FACS analysis from E15 FL from *Flt3*$^{+/+}$ and *Flt3*$^{ITD/ITD}$ mice. Numbers in the graph represent mean frequencies of total FL cells from 7-9 mice of each genotype from 3 independent experiments. There were no significant differences in the frequency of MPPs between *Flt3*$^{+/+}$ and *Flt3*$^{ITD/ITD}$ mice.

(H) Percentage of B220^{+}CD19^{+} cells in E15 *Flt3*$^{+/+}$ and *Flt3*$^{ITD/ITD}$ FL (8-9 FL of each genotype).

(I) Percentage of Mac1^{low}cKit^{low} cells in E15 *Flt3*$^{+/+}$ and *Flt3*$^{ITD/ITD}$ FL (8-9 FL of each genotype). NS indicates not significant.

(J) Expression of lymphoid affiliated genes in LSKFlt3^{+}CD48^{+}150^{-} MPPs from Runx1$^{fl/fl}$VavCre^{-} and Runx1$^{fl/fl}$VavCre^{+} mice (n = 4 mice 4-6 weeks of age per genotype). Error bars represent SEM.

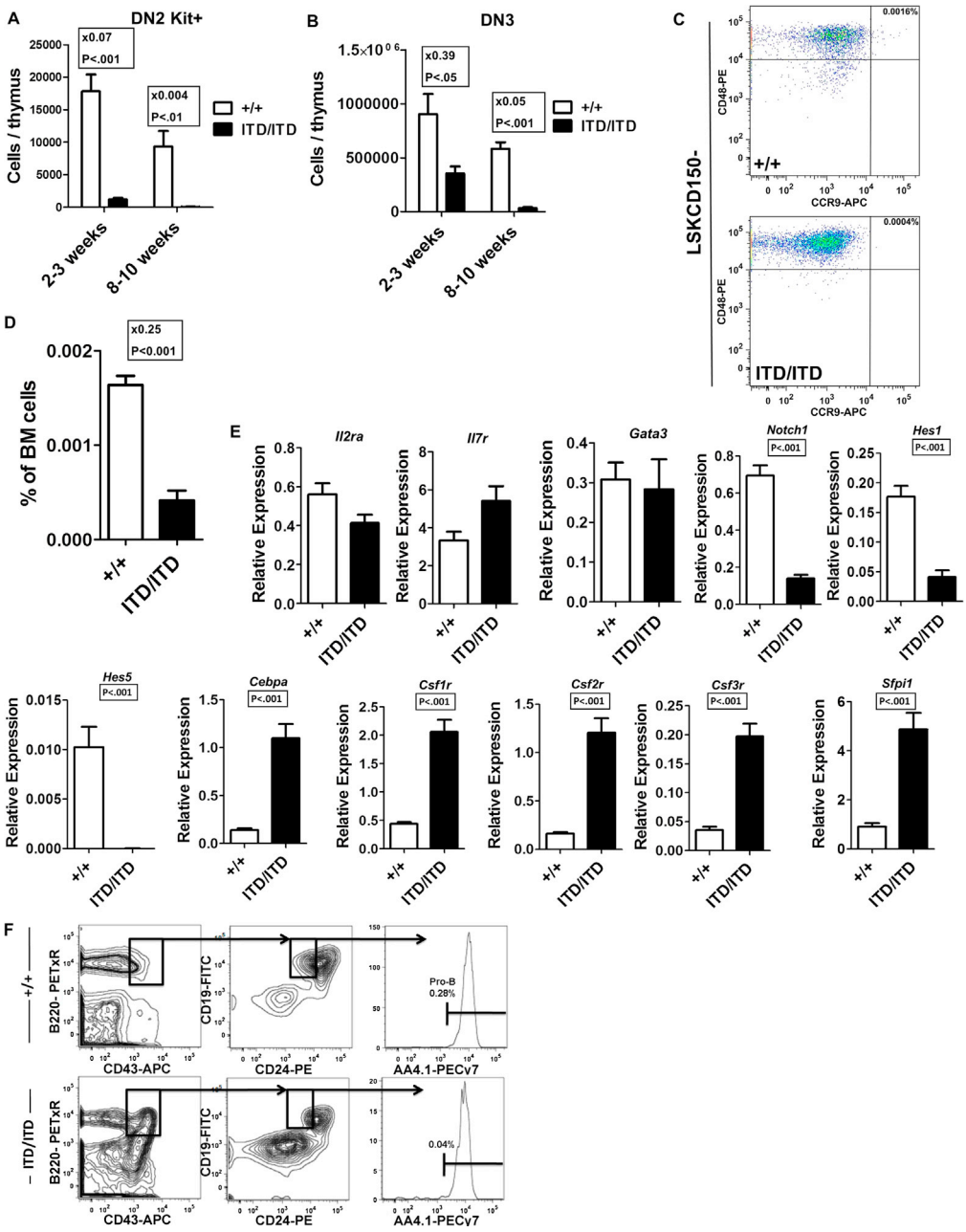

Figure S3. Early T and B Cell Progenitors Are Suppressed and Myeloid Biased in *Flt3*$^{ITD/ITD}$ Mice, Related to Figure 3

(A and B) Progressive loss of DN2Kit^{+} (A) and DN3 (B) thymocyte progenitors in *Flt3*$^{ITD/ITD}$ thymus (mean (SEM) values from 7-8 mice of each genotype at indicated ages in 3 independent experiments).

(C) Representative FACS profile demonstrating loss of Ccr9 expression on the cell surface of LSKCD150^{-} cells in *Flt3*$^{ITD/ITD}$ mice.

(D) Quantification of Ccr9 positive LSKCD150^{-}CD48^{+} cells in *Flt3*$^{+/+}$ and *Flt3*$^{ITD/ITD}$ BM (mean (SEM) values from 5-6 mice of each genotype analyzed at 6-8 weeks of age).

(E) Lineage-affiliated gene expression analysis of DN1 thymocytes from *Flt3*$^{+/+}$ and *Flt3*$^{ITD/ITD}$ mice (mean (SEM) expression, 2 mice per genotype; 3 separately sorted replicates per mouse).

(F) Representative FACS analysis showing gating strategy for identification of pro-B (Lin^{-}B220^{+}CD19^{+}CD24^{mid}AA4.1^{+}) cells in *Flt3*$^{+/+}$ and *Flt3*$^{ITD/ITD}$ mice (percentages are relative to total bone marrow cells). Error bars represent SEM.

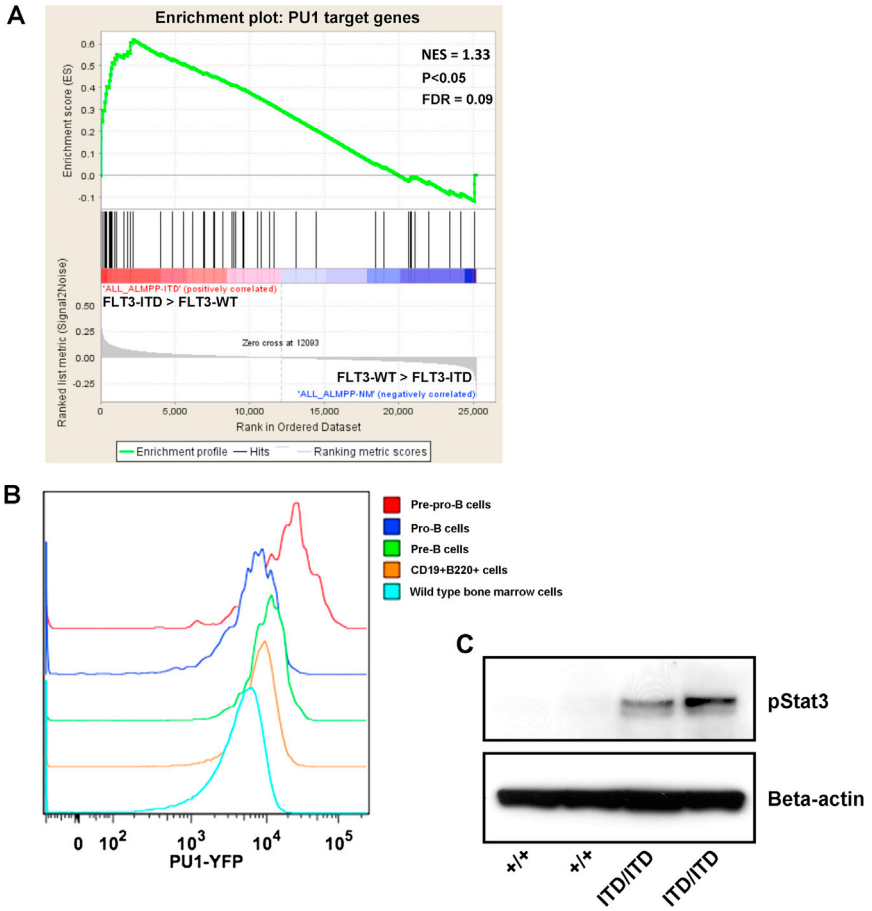

Figure S4. Involvement of Pu1 Upregulation in the Myeloid Bias of *Flt3*$^{ITD/ITD}$ Progenitors, Related to Figure 4

(A) Gene set enrichment analysis demonstrating upregulation of Pu1 target genes in Lin$^-$CD34$^+$CD38$^-$CD90$^-$CD45RA$^+$ cells from *FLT3-ITD* mutated human AML (n = 8) relative to *FLT3-WT* counterparts (n = 18).

(B) Representative FACS analysis of Pu1-YFP expression levels during early B cell commitment demonstrating marked downregulation of Pu1 expression at the pre-pro-B to pro-B transition. Representative of 2 experiments.

(C) Western blot showing increased pStat3 activation in the BM of *Flt3*$^{ITD/ITD}$ mice in comparison with *Flt3*$^{+/+}$ BM. The blot shown is representative of two independent experiments.